Non - Linear Load and Deformation Analysis of Elastomer Piston Seals Using MSC/NASTRAN

S. A. BRADLEY, SENIOR ENGINEER
COMPUTER AIDED ENGINEERING

ALLIED SIGNAL CORPORATION
BENDIX AUTOMOTIVE SYSTEMS GROUP
(NORTH AMERICA)

ABSTRACT:

An investigation of MSC/NASTRAN's capability to model the non-linear behavior of a rubber pumping cup seal. The study limits itself to include only non-linearities caused by large displacement and multiple contact effects. The seal's material behavior is assumed to be linear. This is in accordance with empirical test data and the strain magnitudes encountered. Good correlation with available empirical data is obtained. Results are used to indicate tendencies of the design which contribute to flawed or inadequate performance. A redesign is investigated and recommended.

INTRODUCTION/BACKGROUND:

As in many other industries, today's automotive brake systems rely on extensive use of rubber components. Until recently, the design of rubber components, especially pressure sealing systems, has been essentially black magic. The use of cut and try methods has, to date, been unable to effectively improve the design's performance. The primary reason for this is the inability to actually see and therefore understand the seal's operation. Because of this, seal design has been performed based on personal experience and opinions which are usually biased. Use of computer simulation would seem to be ideally suited for this application, but effective deployment has just started to be realized. This study is only a part of an ongoing effort to establish an accurate and proficient method to assist in the design of rubber components. It represents a baseline investigation of a production sealing system in order to quantify the capabilities and applications of this now ever widening niche of computer analysis.

The sealing system chosen to be analyzed is utilized in a Bendix brake master cylinder program. The system's basic assemblage of components consists of a rubber seal, a fiberglass reinforced nylon sleeve and land, and an aluminum piston. The entire assemblage mentioned is shown in figures (1 & 2). Proper assembly of the system has the seal stretched over the piston and the O.D. lip of the seal tucked into the sleeve. The primary land then completes the assembly by sliding down the piston and trapping the seal.

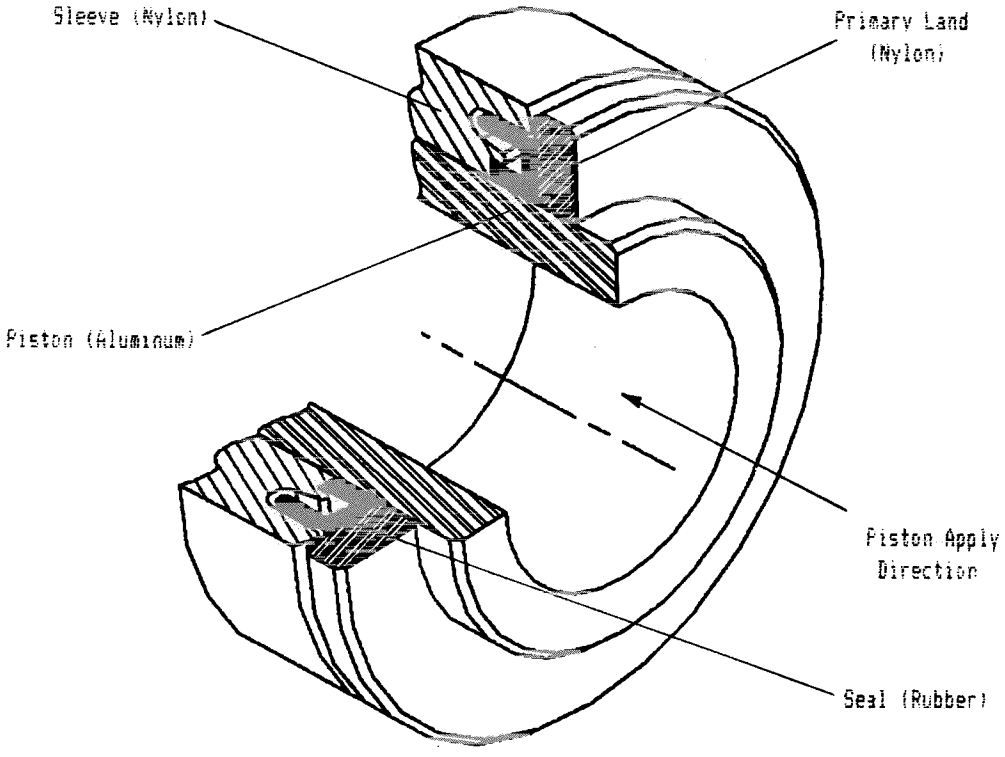

-- Figure 1 --
Assembled Sealing System Showing Major Components

The major responsibility of the design is to allow for proper sealing of the brake fluid during piston application and subsequent pressurization. A normal piston apply stroke would move the piston into the sleeve. Conversely, the return stroke moves the piston out of the sleeve. Knowing this it should be obvious that area (A), denoted in figure (2), will be pressurized during a normal piston apply. This pressurization will not occur, however, until a series of holes (compensation holes) in the piston are covered. The compensation hole's primary purpose is to adjust for possible volume expansion/contraction due to various effects. Another important feature of this seal design is the function

of the O.D. lip. Proper operation of the seal dictates that the O.D. lip allow fluid to flow back into area (A) on the return stroke. This reduces the chances of a vacuum being created during a return stroke and allows for better compensation on rapid piston returns.

Along with maintaining the proper operation of the assembly, three major issues quantify the performance of of this particular design;

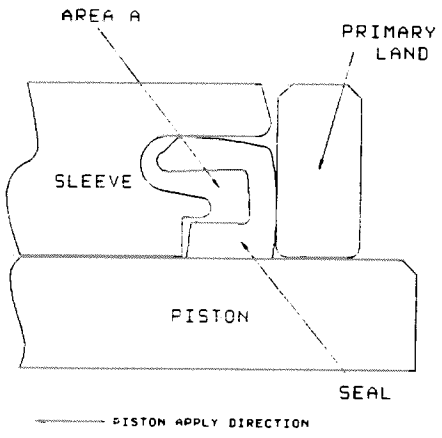

-- Figure 2 --
Assembled Sealing System

1) The reduction of piston travel required to facilitate a rise in pressure in the system (commonly refered to as comp. loss).

2) The reduction in the amount of fluid displacement gained due to seal expansion during a normal piston apply.

3) The reduction of noise generated during a normal return stroke (a problem which appears in the current design).

By investigating the behavior of this seal and addressing the design issues that are unique to its use, it will be possible to evaluate the effectiveness of using FEA as a tool in the design of rubber components.

ANALYSIS PROCEDURE:

This analysis is a non-linear static solution. Non-linearities in the solution are due to the changes in geometry and boundary conditions. No allowances are made for non-linear material behavior since the strains in the design are not expected to exceed 20% and the material's stress/strain relation is linear up to this level. The analysis focuses on the seal design only. No changes are made in the confining geometry, which is considered ideally rigid. Furthermore, the geometry is considered to be nominal and perfectly centered. The FEA solver, MSC/NASTRAN (version 65C, solution 66), is utilized throughout the analysis. Solving is performed on an IBM mainframe using the VM/CMS operating system.

The model used is shown in figures (3 & 4). It is comprised of 4 separate pieces of geometry (the seal, piston, land, and sleeve as denoted in figure (1)). Representation of the seal and the associated confining geometry is accomplished by employing solid brick (8-noded CHEXA) and quadrilateral shell (4-noded CQUAD)

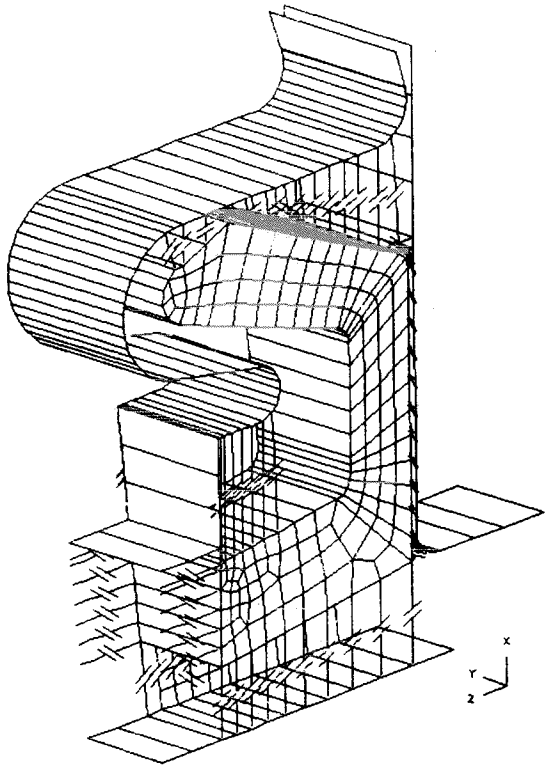

-- Figure 3 --
Finite Element Model Used to
Simulate Production Sealing System

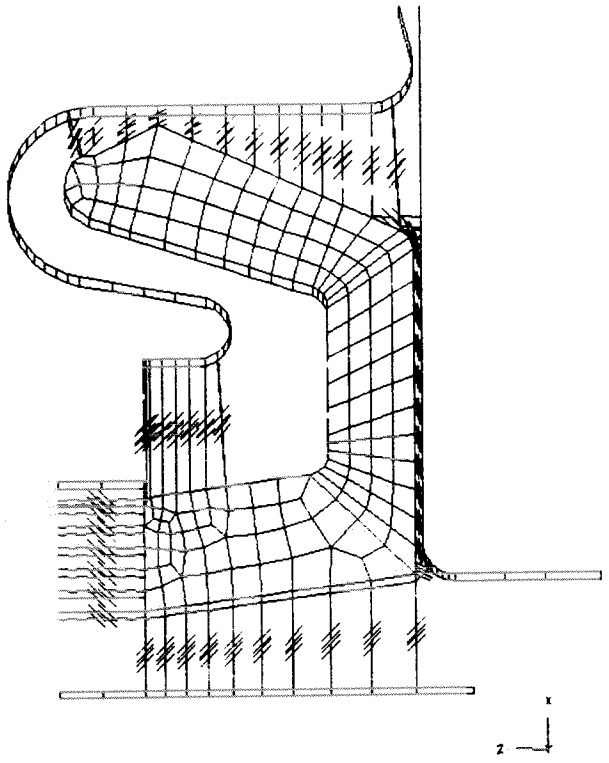

-- Figure 4 --
Profile of Finite Element
Model Shown in Figure 3

elements, respectively. The motion of each piece is independent of the others with the exception of where contact is expected. At the anticipated contact interfaces, the appropriate geometry is attached through the use of node to node contact elements (CGAP). Axi-symmetrical conditions are valid and employed. The geometry is defined in a cylindrical coordinate system which is centered on the piston axis. Use of the cylindrical coordinate system provides easy application of the axi-symmetric boundary conditions (Θ-translations and rotations in the R-Z plane). Additional restraints are applied to the confining geometry in the R and Z directions. Simply put, the seal geometry is free to translate in the R and Z directions unless constrained by contact. The confining geometry is completely restrained. Motion of the confining geometry is restricted to the amount specified by the user as an enforced displacement.

The position of the initial geometry is dependent upon the expected contact. The seal geometry is defined in its free state but the confining geometry is aligned according to the seal's free state and the expected contact with the seal. Nodal positions on the seal's surface are then projected to the confining geometry surface. This dictates the mesh on the confining geometry and properly aligns the gap element coordinate systems. At this point it should be obvious that the seal geometry is "suspended" in the R-Z plane by the gap

elements that are attached to the confining geometry. It should also be apparent that the elements that comprise the confining geometry are not actually used in the simulation of the physical system. They are only added to assist in the visualization of the confining geometry. One additional note, two parts of the sleeve geometry contact the seal at different angles which makes the projection of the contact points impossible. This problem is resolved by having one of the contact areas become a so-called "phantom" or invisible part. In other words, the nodes defining the contact are not contained in any elements. The axial contact of the sleeve is modeled this way and is refered to as the "bumper".

Loads applied to the configuration described above can be categorized into two types; assembly and/or operational. Assembly loads are those incurred through the geometric interaction of the components as they are assembled. Operational loads are developed by piston motion and/or an internal pressure increase. They are applied after the system is assembled. Since this is a non-linear or path-dependant solution, the actual assembly logic is very critical. Operational loads will not produce consistent results if the assembly procedure is altered, but it is impossible to account for all the slight variations that might occur in normal production. Consequently, some assumptions about the actual assembly method are conceded. Assembly is accomplished in 4 phases as described in figure (5).

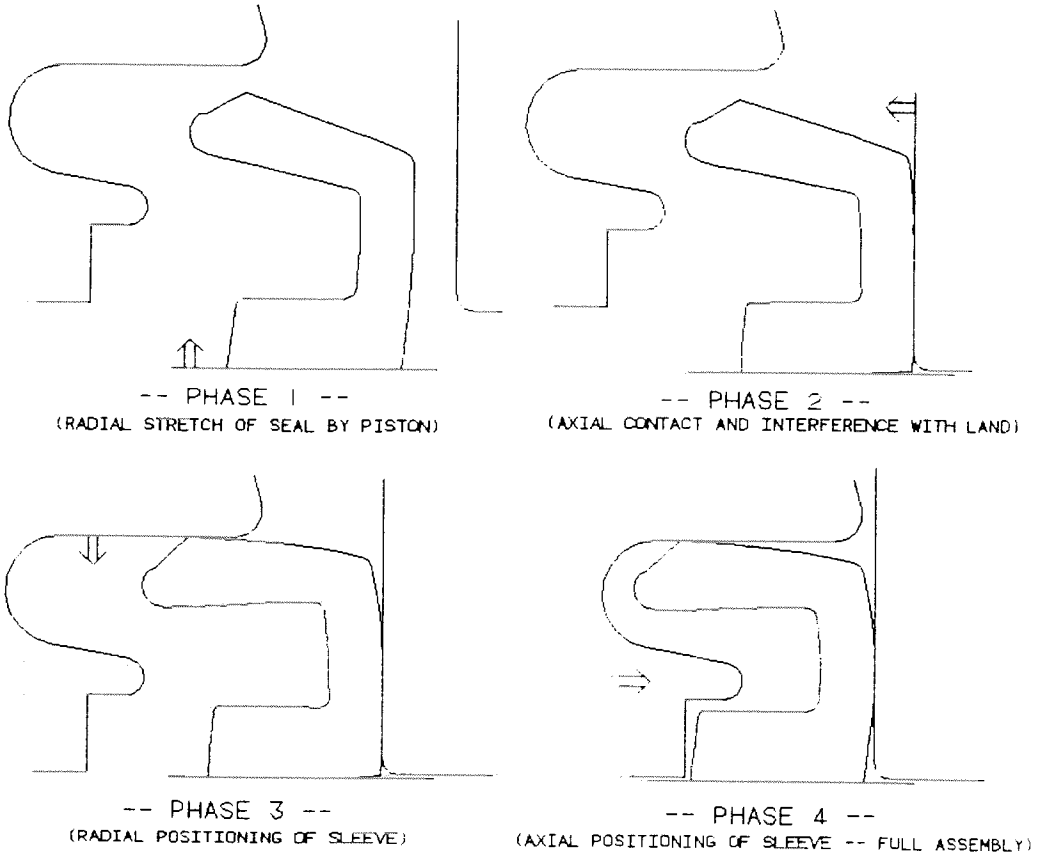

-- Figure 5 --
Breakdown of the Major Phases Used to Simulate Assembly

Production procedure would be to hold the piston, seal, and land in one hand and have the sleeve in the other. The two pieces would then be pushed together to complete the procedure. However, the O.D. lip of the seal presents an interference fit with the contour of the sleeve. During production assembly, it is hoped that the geometry and force/stiffness relationships of the design will force the O.D. lip to tuck into the sleeve. However, due to inadequacies in the formulation of the gap elements (CGAP) in version 65C of MSC/NASTRAN, modeling of this interference could not be accomplished. Therefore, it is assumed that the O.D. lip of the seal does in fact slip into the sleeve. The separation of the sleeve assembly into phases 3 and 4 reflects this assumption. Actual investigation of this seal/sleeve interference has been handled by using a kinematic comparison.

Movement of the separate pieces of geometry is accomplished through the use of SPC's. A dummy load (small in magnitude) must be applied to satisfy software checks but, other than this, no load is placed on the configuration. Initial movement of the geometry shown in figure (3 & 4), merely moves the sleeve and land geometries away from the seal so as not to interfere during the seal stretch stage. It should be mentioned that until the seal is contacted, it is restrained in the Z direction by the combined stiffness of the open gap elements. This alone does not provide adequate restraint of the seal and convergence is difficult to obtain. Therefore a single node on the seal geometry is held until contact with the piston and a subsequent frictional load is developed. This restraint is then removed and the solution is allowed to iterate in a so-called "relaxation" step.

From this point positioning of the remaining geometry is rather straight-forward with the exception that initial contacts and the initiation of slippage must be stepped into slowly. A preferred approach is to divide the major motions into subcases, then account for convergence problems by varying the INC parameter on the NLPARM card. Not only does this organize the assembly phases, but it also separates difficult steps from easier ones which allows for quick and accurate restarts. Once assembly is completed, actual operational loading can be applied to the model. These loadings are performed as restarts from the assembled data base to preclude the resolving of the assembly procedures. The actual assembly procedure is listed in figure (6).

As for actual run data, most of the specific stiffnesses, convergence rates, solution strategies, etc. were derived in earlier benchmark studies. Actual development of this data can not be included in the scope of this report. Instead, the necessary inform- is briefly summarized.

The solution strategy ITER 1 was chosen since it proved to be the most robust method. Time and computer resources were usually wasted if the solution was allowed to find the most efficient strategy. Convergence criteria was developed from two separate observations. The first being a failure to obtain global equilibrium. This was closely related to having the DLMAG convergence term reaching a value of 1.0E-3 or below. The second, was the realization that the displacement criteria in MSC/NASTRAN uses the stiffness matrix as a weighting function. For the ITER 1 solution strategy, this seems

ITERATIONS OF SEAL ASSEMBLY		
Step 1)	Primary Land Removal	2 Iterations
Step 2)	Sleeve and Bumper Removal	2 Iterations
Step 3)	Initial Piston Contact	2 Iterations
Step 4)	Full Piston Contact	5 Iterations
Step 5)	Piston to Nominal Radius (Denoted as Phase 1)	2 Iterations
Step 6)	Relax Seal Stabilizing SPC's	2 Iterations
Step 7)	Move Land to Nominal Radius	1 Iterations
Step 8)	Move Land To Just Before Contact	1 Iterations
Step 9)	Full Land Contact and Push (Denoted as Phase 2)	7 Iterations
	Relax Solution	1 Iterations
Step 10)	Sleeve To Just Before Contact	1 Iterations
Step 11)	Sleeve To Nominal Radius (Denoted as Phase 3)	3 Iterations
Step 12)	Sleeve and Bumper To Full Assembly (Denoted as Phase 4)	3 Iterations
	Relax Solution	1 Iterations
		33 Iterations

-- Figure 4 --
Assembly Procedure with the Number of Load Steps Denoted
(load steps are comparable iterations in this figure)

to be inappropriate because the stiffness matrix changes, sometimes drastically, for each iteration. This is backed up by successive solutions and (1,2). Therefore, the solution monitors the residual load and energy and sets their acceptance values at 1.0E-05 and 1.0E-10 respectively. For some cases this criteria is stringent but for most it proved to be warranted in establishing smooth and accurate convergence.

Properties for the gap elements (CGAP) were kept consistent throughout the model. Stiffnesses used for the open and closed conditions were 1.0E-01 (mn/mm) and 1.0E+09 (mn/mm) respectively. The transverse stiffness was set at 1.0E+03 (mn/mm). These stiffnesses

were developed through numerical experimentation and are based on accuracy and convergence rates. (3) cites similar values for a similar problem. The preload placed on the gap elements is as recommended in (4). One important point is that use of initial nodal coincidence in the gap elements was always avoided. Problems with convergence occurred if the nodes defining the gap elements were initially coincident.

The confining geometry was arbitrarily defined, but in order to stay away from possible numerical singularities, the material was kept equal to the seal and the shell thicknesses were assigned values on the order of magnitude of the seal dimensions. It should be noted that the only deformation seen by these elements is due to radial stretching during their placement. However, this deformation alone can produce high strains and, therefore, the radial motions should be kept at low orders of magnitudes so as to preclude possible complications. The seal material properties were assigned 783 psi (5400 mn/mm^2) and (.49) for Young's modulus and Poisson's ratio respectively. Determination of these properties is discussed in the next section.

Since solution 66 was utilized, the AUTOSPC command did not properly restrain the solid element rotations. This was accounted for by use of a SPC1 card for all nodal rotations. LGDISP (large displacement theory) was flagged and the DBNBLKS were assigned 55000 to account for the entire solution (assembly and operational loading). Restarts were made from any subcase's final iteration as long as it converged. Some problems were encountered when iterations inside subcases were used for restart points. When moving geometry the relative translation was input using SPC cards. SPC cards were utilized because of the author's preference, but use of either SPC or SPCD cards will result in the same model response.

EMPIRICAL BACKGROUND:

The accumulation of empirical data for this study was two fold. First, information on the material's stress-strain behavior, frictional coefficients and assembly procedure was required in order to match the physical situation. Second, correlation data such as force-displacement information, outlines of assembly system, and actual engineering experience and observations were required to determine the adequacy of the solution.

As for input information, samples of the seal material were tested at Bendix's material laboratory. Two stress-strain curves were developed which are provided in figures (7 & 8). They represent the material behavior to failure and within the 50% strain range. Curves for engineering and true stress-strain are provided in the smaller range. It should be noticed that the response is linear in the lower ranges. A Young's modulus of 783 psi was calculated from the true stress-strain curve. This is used in conjunction with a Poisson's ratio of .49 which is a close estimate of the usually presumed value of .5 and what has been established in (5). Frictional coefficients for the seal/piston interface were derived by measuring the force required to push the piston into the sleeve (4.2 lbs). This was then compared to the FEA obtained stretch force which the seal exerts on

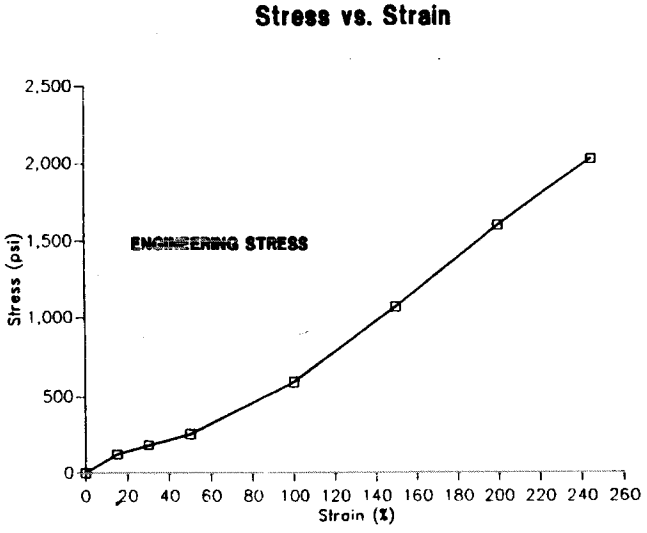

-- Figure 7 --
Stress-Strain Curve For Rubber Test Specimen. Curve Includes Failure of the Specimen. Area Reduction is Not Accounted.

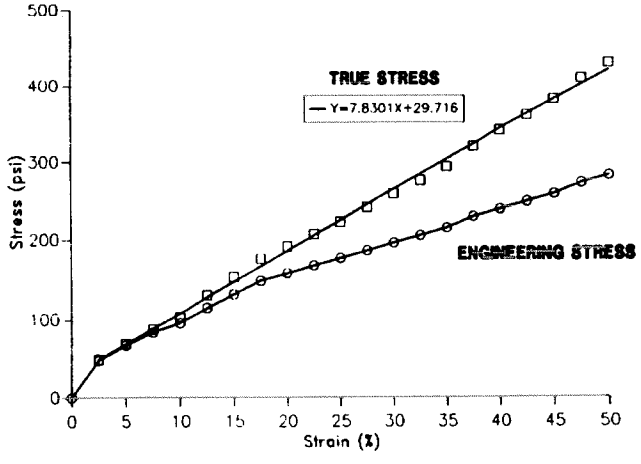

-- Figure 8 --
Stress-Strain Curve For Rubber Test Specimen. Similar to Curve Shown in Figure 7. Highlights the 0-50% Strain Region and Provides Both Engineering and True Stress Curves.

the piston. This coefficient was then correlated by predicting the force to push the piston out of the sleeve (≈6.0 lbs). The seal/nylon sleeve and land interface coefficient was obtained in a similar manner. It is believed that excellent correlation with this empirical data was obtained, however, it has been determined through recent tests that this data is specific to certain configurations. The discussion of this, is beyond the scope of this paper, but it should be noted that frictional data for this type of analysis is not only very critical but is somewhat undefinable and elusive. This is due to of all the possible variations in geometry, brake and/or assembly fluid properties, and/or application speed.

Frictional data provided some correlation of the solution but additional data was made available by making a mold of the assembled system. Figure (9) shows the comparison between the FEA predicted shape and that obtained from the mold. Very little, can be derived from this information because the geometry is not an exact representation and the final shape is highly dependent upon assembly method. What can be seen and correlated is the

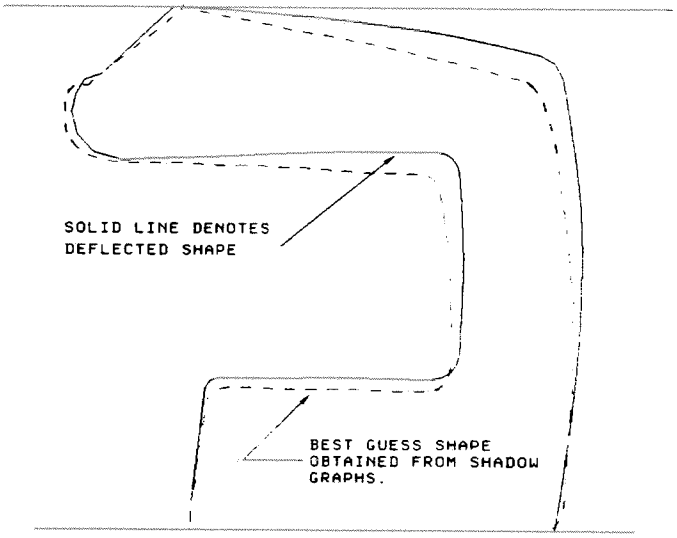

-- Figure 9 --
Comparison of Predicted Seal Profile to the Profile of the Assembled Seal Obtained by Using a Silicone Gel Mold.

general shape of the seal. Note that both exhibit the arching of the vertical portion of the seal. Also, the front face of the I.D. lip is merely rotated as the I.D. lip is stretched. This results in a similar, "snow-plow" type, leading edge. Also similar is the contact of the O.D. lip and the sleeve. Both show the tendency for the O.D. lip to bend down instead of locally deforming at the point of contact.

After considering the scope of this study and discussing the results with the development engineers it was determined that the information available provided adequate correlation to the model. This conclusion was upheld when this same model was used to investigate a recent issue on a similar seal.

DESIGN INVESTIGATION:

Results from the simulation of the current sealing system for the assumed assembly and selected operational loads are shown in figures (10-16). Figure (10) provides an overview of the major steps in the assembly. Notable in figure (10d), is the indication that the I.D. lip's leading edge will buckle as the seal is forced down the piston by the land. It should be reported that this is believed to be localized buckling and should not affect the global response of the seal. It is characterized by the occurrence of negative diagonal terms in the matrix, for rows associated with the buckled region. Care should be taken when reviewing the results of the post-buckled

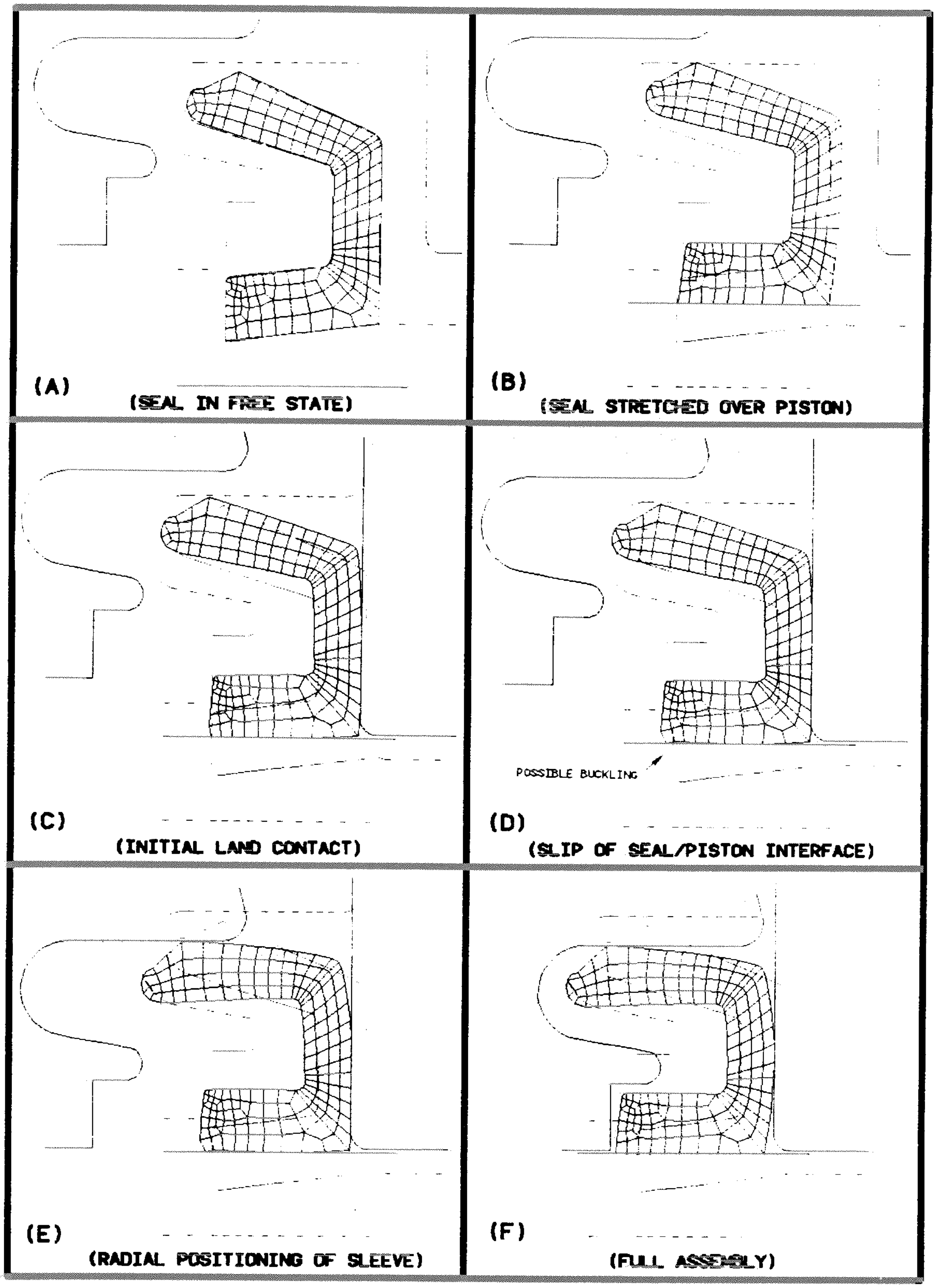

Figure [illegible]
Overview of the [illegible] Assembly [illegible]

response. This occurrence is relieved once the piston is moved so as to reduce the frictional forces that produced the buckling. It does provide an explanation of observed noise during normal return strokes in actual parts. Also, in figure (10f), note that during the assembly of the system, the seal's vertical portion is deformed such that it bows away from the land. This provides correlation to lab tests and opens up the possibility of increased fluid displacement during a brake apply due to the extra volume available for seal extrusion. Conversely, there is adequate space available above the O.D. lip for proper replenishment. This space, in conjunction with the O.D. lip stiffness, determines the pressure required to provide replenishment when required by the

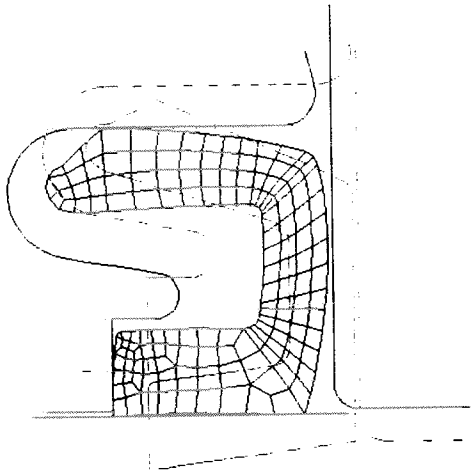

-- Figure 11 --
Predicted Response to a Piston Apply Stroke that Produces Slippage at the Seal/Piston Interface

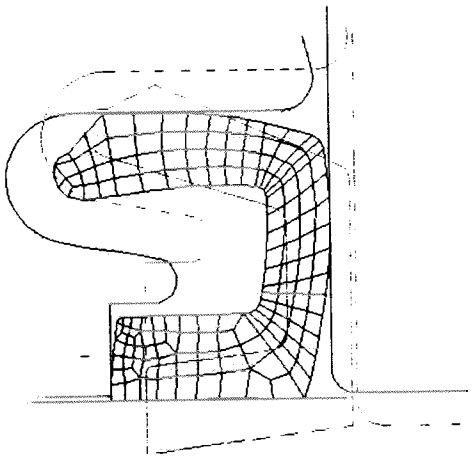

-- Figure 12 --
Predicted Response due to a 7 psi Pressure Increase. Contact to the Land is Re-Established

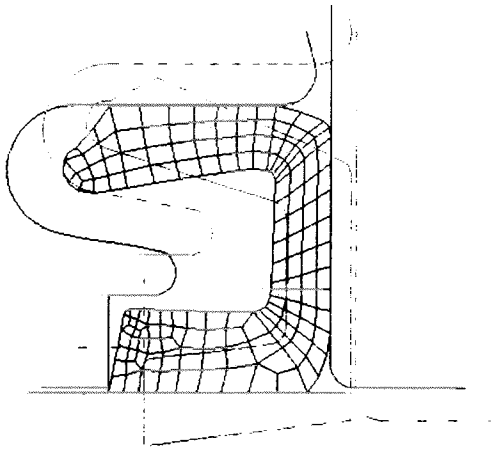

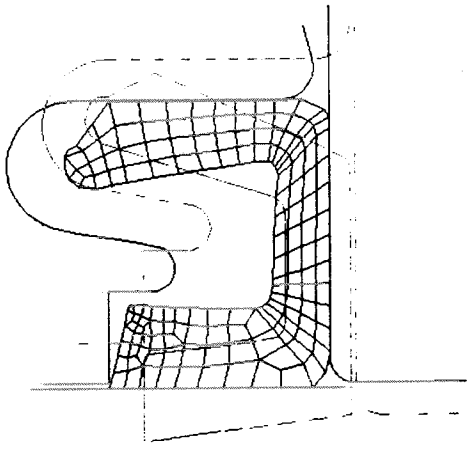

-- Figure 13 --
Predicted Response under 100 and 200 psi Pressure Application

system. If excessive contact of the O.D. lip with the sleeve restrict this area, proper replenishment will not occur.

Figures (11-13) show the expected seal response to two types of operational loads; piston movement and internal pressure increase. Due to various complications, the two loads are treated as separate occurrences. The response as a result of a piston apply is shown in figure (11). Here the piston is pushed into the sleeve (simulating a normal brake apply) until the I.D. lip contacts the sleeve and experiences slippage at the piston/seal interface. Notable is the bowing and subsequent liftoff of the I.D. lip and the distance the I.D. heel travels from its original position. The first response is due to the geometry of the front face of the I.D. lip and provides excellent correlation to engineering observations. Figure (14) provides a graphical explanation for this occurrence. The second response is a primary design objective since it directly affects the amount of piston travel required to cover the compensation holes.

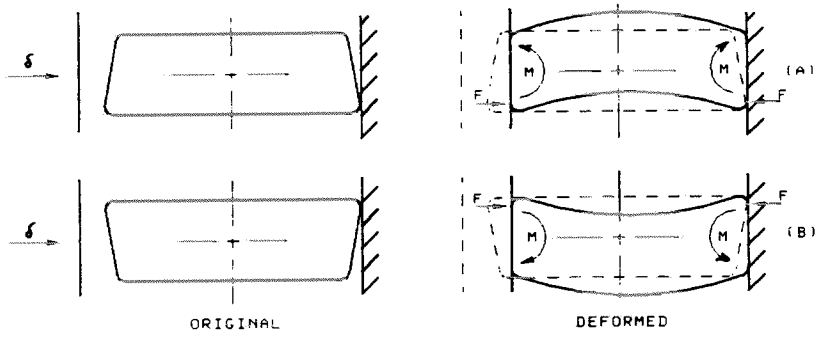

-- Figure 14 --
Graphical Depiction of How the Geometry of the Front Face of the I.D. Lip Dictates the Action of the Lip

Figures (12 & 13) show the seal's expected response when subjected to fluid pressure. The pressure application occurs after the piston motion, previously described, is completed. The two figures depict the seal's response @ 7, 100 and 200 psi. The 7 psi load represents the fluid pressure required to force the seal to contact the land. From here, pressure is steadily increased to 200 psi. Figure (13) represents the expected response @ 100 and 200 psi. Results at these pressures are reported, but once the fluid pressure exceeds 60 psi, instabilities in the solution start appearing. These instabilities are again characterized by the occurrence of negative terms on the diagonal. This occurrence, believed to be local in nature (even termed local crippling by some support staff), does however, coincide with the seal material strains exceeding 20%. A discussion of this is beyond this forum. Further work is needed to nail down the affect of the occurrences and therefore the results of these stages are reported for comparison purposes only.

Due to the nature of this study and since rupture of the seal is not a primary design concern, an in depth investigation of the stress fields in the seal is not included in this discussion. A sample of the stresses seen in the study is included in figure (15) which presents the three normal stress fields expected in the seal upon assembly.

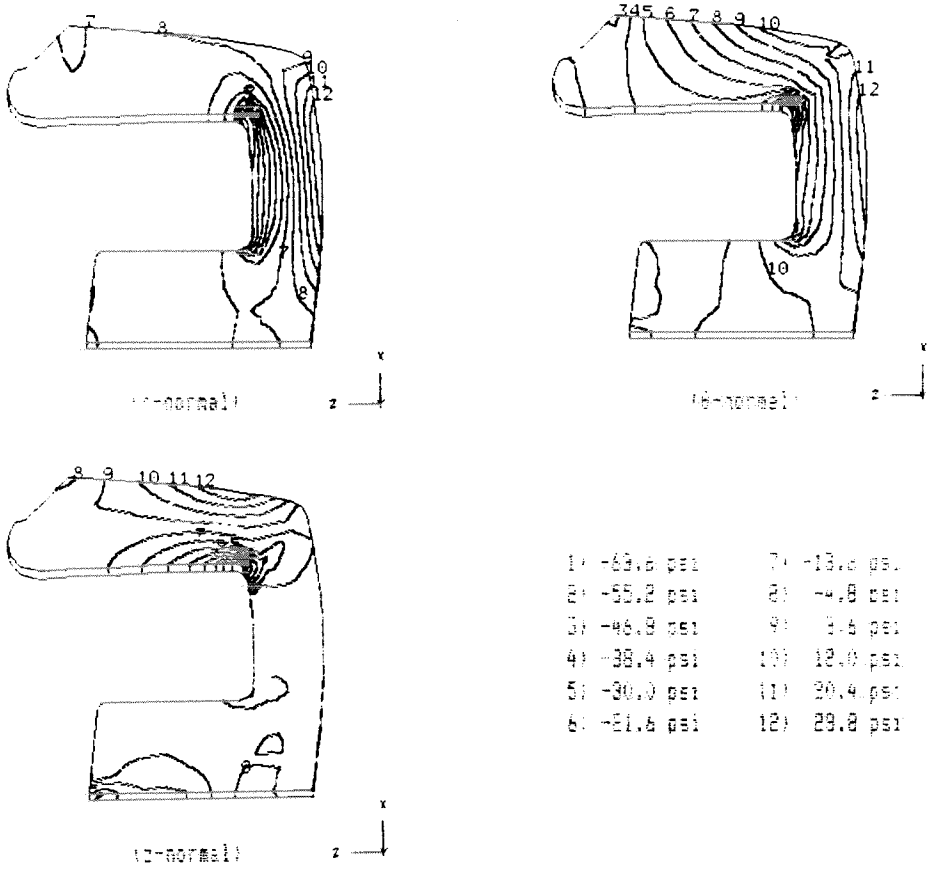

-- Figure 15 --
Typical Stress Fields Expected in Seal Upon Assembly
(normal stresses shown are reference to the R, θ, Z system)

As a final piece of information on the current design, figure (16) shows a comparison of the pressure face in its undeformed position and after the 200 psi application. From this, the expected extrusion tendencies can be seen.

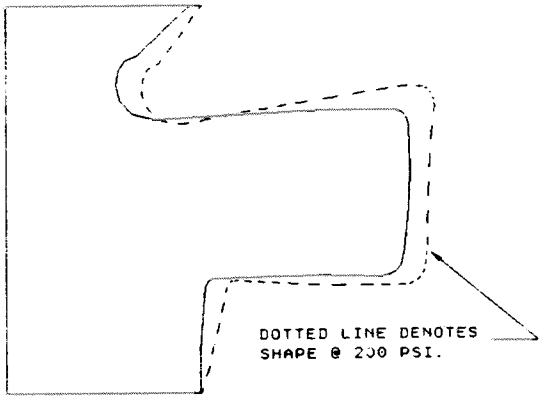

-- Figure 16 --
Comparison of the Affects that a 200 psi Pressure increase has on the Seal Profile (solid line denotes assembled configuration)

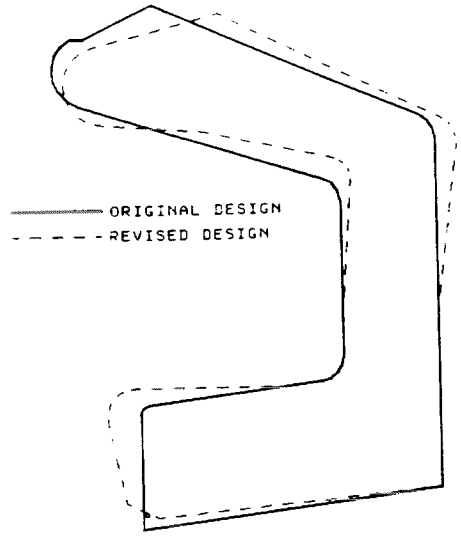

-- Figure 1" --
Revised Seal Profile Overlaid onto
Production Profile, Both are
shown Their Free State.

DESIGN ENHANCEMENT:

Review of the results for the current design produced several ideas on improvement of the seal's geometric profile. The most promising seal profile developed is shown in figure (17). It is shown overlaid on the original geometry for visual comparison. Summarizing the major changes made;

1) The back of the seal is canted to provide a flusher fit once the seal is squeezed into the piston/sleeve confinement. This will reduce the area available for extrusion, thus, decreasing the amount of fluid required for pressurization.

2) The I.D. lip is extended so as to create an interference fit between the sleeve and land. This will also reduce the area available for extrusion and provide a more controlled seal response during operation.

3) To combat the adverse affects of item 2, the nose of the I.D. is slanted such that initial contact with the sleeve will occur on its outer most radius (refer to figure (14)).

4) The leading edge of the I.D. lip is chamfered and moved radially outward to reduce the stretch force on the piston. This was aimed at reducing the noise generated during return strokes by alleviating the local buckling.

5) The hoop stiffness of the O.D. lip is increased by adding rubber but its bending stiffness is decreased by reducing its section at the intersection to the seal's back. This improves the replenishment characteristics and provides easier installation into the sleeve.

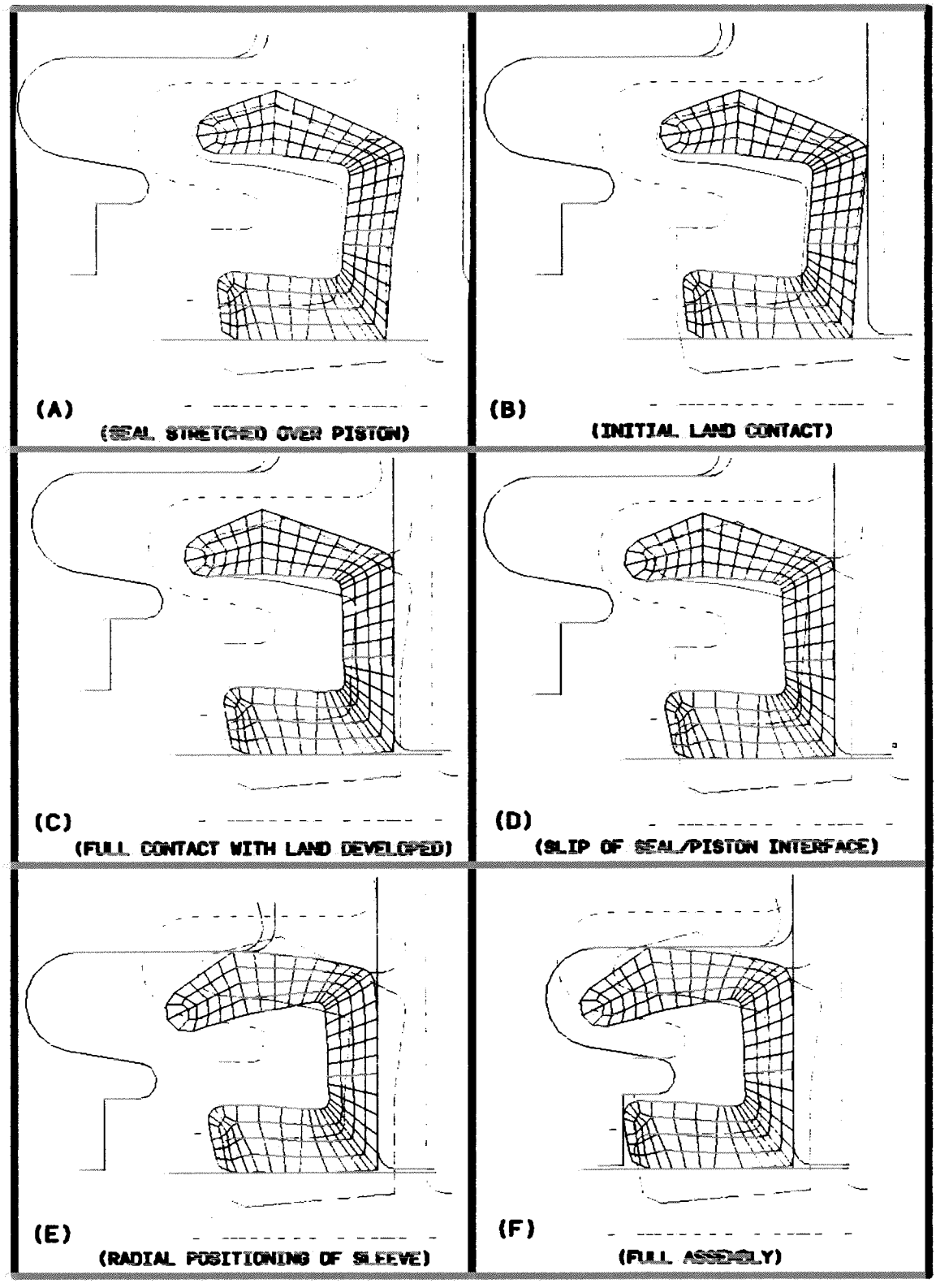

-- Figure 18 --
Overview of the Major Assembly Steps (revised design)

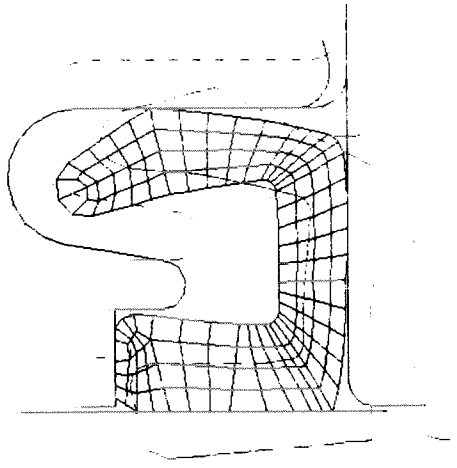

-- Figure 17 --
Predicted Response to a Piston Apply that Produces
Slippage at the Seal/Piston Interface (revised geometry)

Figures (18-20) show the predicted response of the revised seal for the major assembly stages and operational loads. Figure (21) provides a comparison of the I.D. heel liftoff for both designs and figure (22) shows the relative change in the pressure face. This is directly comparable to figure (16). Further manipulation of this data is shown in figure (23). Figure (23) represents a numerical comparison of the fluid displacement lost to the extrusion of each design. The graph is normalized to the amount lost in the current design at 200 psi.

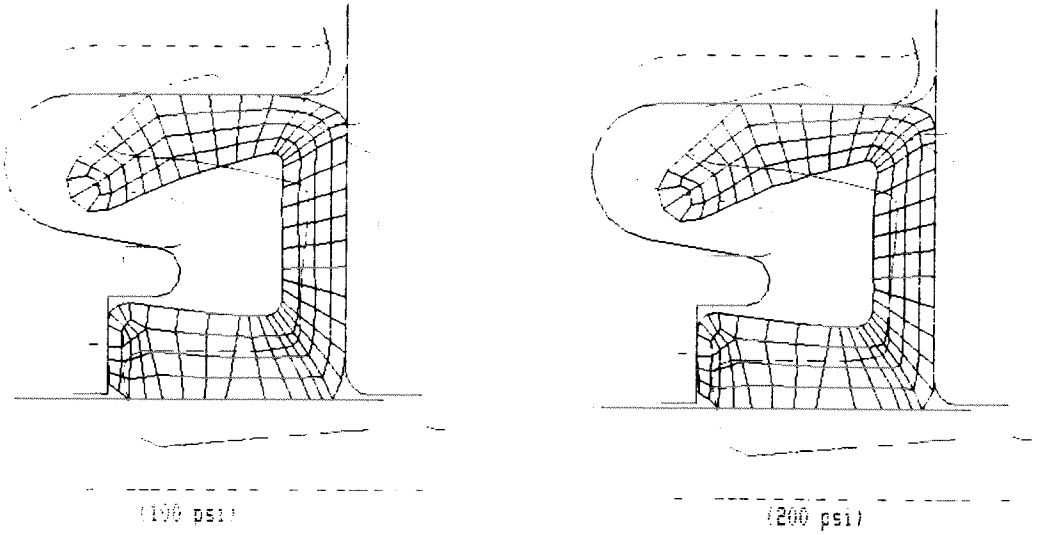

-- Figure 20 --
Predicted Response under 100 and 200 psi Pressure Application
(revised geometry)

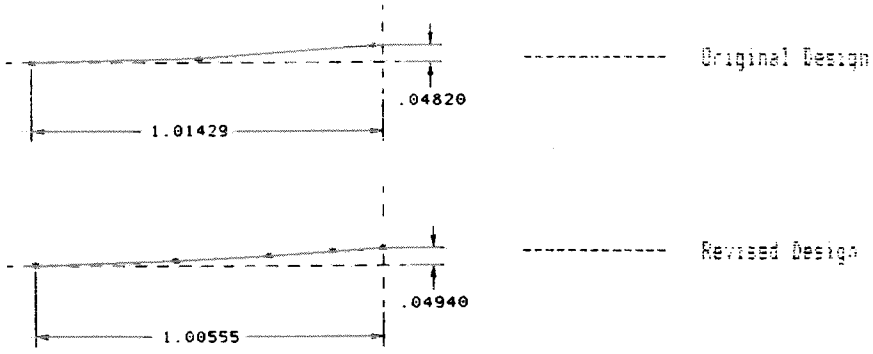

-- Figure 21 --
Comparison of the Expected I.D. Heel Liftoff Upon
a Normal Piston Return (liftoff values are given in mm)

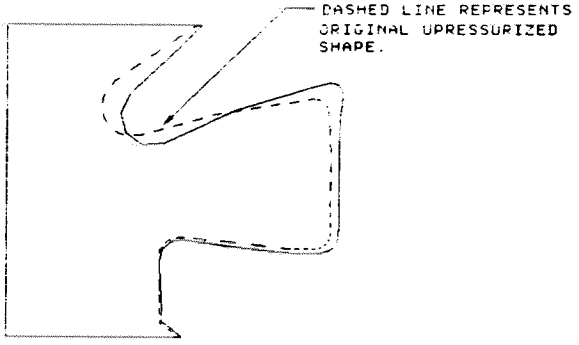

-- Figure 22 --
Comparison of the Affects that a 200 psi Pressure
Increase has on the Revised Seal Profile (dashed line
denotes assembled configuration)

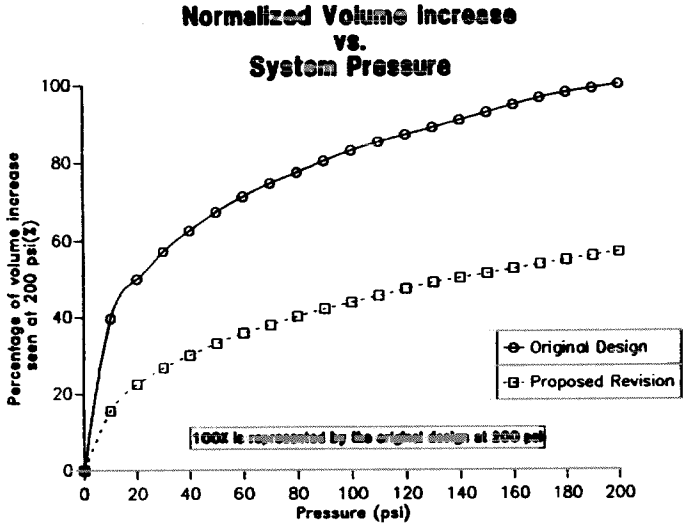

-- Figure 23 --
Comparison of Expected Volume Expansion for Both Seal Profiles

CONCLUSIONS:

By evaluating the application of non-linear finite elements to actual production components, this study has established a baseline for future seal design at Bendix. Use of the techniques on a current, well established, design provided support for their accuracy and highlighted problems with the method used. Once developed and honed, use of the method to identify and resolve problems found in the chosen system helped identify the capabilities and the possibilities for its deployment.

Additional work is required in many aspects of the method. First, formulation of the gap (CGAP) elements should be investigated to determine a method to model the interaction of contacting curved surfaces. Second, the frictional force/displacement curve used in the gap (CGAP) element should have a smoother transition through its origin. The abrupt change that currently exists causes severe convergence problems when and if the direction of slip is altered. A possible solution for this could be the addition of a NOLIN element with a specially prescribed transition curve over the range in question. As a final note, effort should be focused on extending this solution technique to include large strain effects.

ACKNOWLEDGEMENTS:

The author would like to extend his thanks to the designers and engineers in the Bendix master cylinder groups especially to J. Steer, G. Matuzak, and R. Zander for their time and experience. Gratitude is also extended to the MSC/NASTRAN support groups and Bendix's computer aided engineering group for their help and expertise.

REFERENCES:

1. Lee, S. H., "Rudimentary Considerations for Effective Convergence Criteria in Nonlinear Finite Element Analysis", MSC, pp 1-9.

2. Bathe, K. J., Cimento, A. P., "Some Practical Procedures for the Solution of Nonlinear Finite Element Equations", Computer Methods in Applied Mechanics and Engineering, 1980.

3. MSC/NASTRAN Application Manual, Section 5, May 1988, pp 1-17.

4. MSC/NASTRAN User's Manual, Section 2.4, March 1983, pp 250-252.

5. Cieslak, J. G., "Material and Geometric Nonlinear Analysis of an Engine Cylinder Gasket using MSC/NASTRAN", 1986.

6. MSC/NASTRAN Application Manual, Section 2.14, June 1983, pp 1-186.

7. Chang, H. H., "On a Numerical Study for Rubber Seals", SAE International Congress and Exposition, 1988.

8. MSC/NASTRAN Material and Geometric Nonlinear Analysis (version 65) (course handbook), July 1989.